



OPEN

Microglial response to experimental periodontitis in a murine model of Alzheimer's disease

Alpdogan Kantarci¹, Christina M. Tognoni^{2,3}, Wael Yaghmoor¹, Amin Marghalani¹, Danielle Stephens¹, Jae-Yong Ahn^{2,3}, Isabel Carreras^{2,3,5,6} & Alpaslan Dedeoglu^{2,3,4,6}✉

Periodontal disease (PD) has been suggested to be a risk factor for Alzheimer's disease (AD). We tested the impact of ligature-induced PD on 5xFAD mice and WT littermates. At baseline, 5xFAD mice presented significant alveolar bone loss compared to WT mice. After the induction of PD, both WT and 5xFAD mice experienced alveolar bone loss. PD increased the level of Iba1-immunostained microglia in WT mice. In 5xFAD mice, PD increased the level of insoluble A β 42. The increased level in Iba1 immunostaining that parallels the accumulation of A β in 5xFAD mice was not affected by PD except for a decrease in the dentate gyrus. Analysis of double-label fluorescent images showed a decline in Iba1 in the proximity of A β plaques in 5xFAD mice with PD compared to those without PD suggesting a PD-induced decrease in plaque-associated microglia (PAM). PD reduced IL-6, MCP-1, GM-CSF, and IFN- γ in brains of WT mice and reduced IL-10 in 5xFAD mice. The data demonstrated that PD increases neuroinflammation in WT mice and disrupts the neuroinflammatory response in 5xFAD mice and suggest that microglia is central to the association between PD and AD.

Alzheimer's disease (AD) is an age-associated neurodegenerative disorder and the most common type of dementia. AD is clinically characterized by a progressive decline in memory, language, and learning capacity, ultimately ending in death¹. The pathological hallmarks of AD are the formation of extracellular plaques composed primarily of amyloid-beta peptide (A β) and intraneuronal neurofibrillary tangles (NFT) of hyperphosphorylated tau protein, which lead to the loss of neuronal synapses and neuronal degeneration^{1,2}. AD pathology is associated with a sustained and unresolved neuroinflammatory response that is characterized by the chronic activation of microglia. In a mouse model of AD, we have recently demonstrated that the inflammatory process is impaired and can be restored by treatment with the agonists of resolution of inflammation³. Under homeostatic conditions, microglia cells are highly branched, surveying the environment for the detection of potential pathological changes. When this occurs, microglia undergo changes in morphology, surface phenotype, and secretory profile in a process referred to as activation⁴. Activated microglia are critical for the phagocytosis and clearance of foreign particles and cellular debris as well as for regulating the immune systems during the inflammatory response^{5–7}. Microglia cells become activated in response to A β accumulation, cluster around A β plaques, and contribute to A β clearance⁸. However, the ability of microglia to clear A β may wane with age^{9,10}. The chronic inflammatory response of microglia to the persistent accumulation of A β contributes to the disease progression by releasing neurotoxic cytokines and reactive oxygen species, which initiate a pro-inflammatory signaling cascade that exacerbates the deleterious effects caused by A β and tau^{8,11}. Recent evidence suggests that plaque-associated microglia (PAMs) form a protective physical barrier around amyloid deposits, compacting amyloid fibrils into a potentially less toxic form, preventing the addition of new A β onto existing plaques, and protecting nearby neurons from A β toxicity¹². Thus, both deleterious and protective effects of AD-induced activated microglia have been described with mounting evidence of the important role that microglia have in AD^{13,14}.

¹Forsyth Institute, 245 First Street, Cambridge, MA 02142, USA. ²Department of Veterans Affairs, VA Boston Healthcare System, Research and Development Service, Building 1A-(151), 150 S. Huntington Avenue, Boston, MA 02130, USA. ³Department of Neurology, Boston University School of Medicine, Boston, MA 02118, USA. ⁴Department of Radiology, Massachusetts General Hospital and Harvard Medical School, Boston, MA 02114, USA. ⁵Department of Biochemistry, Boston University School of Medicine, Boston, MA 02118, USA. ⁶These authors contributed equally: Isabel Carreras and Alpaslan Dedeoglu. ✉email: dedeoglu@bu.edu

Systemic inflammation is capable of inducing neuroinflammation^{15,16}. Chronic inflammatory diseases have been significantly correlated with AD pathology^{17–19}. Thus, the relationship between dissemination of inflammation from other pathologies in distant organs and AD progression is highly plausible. Chronic infections, such as periodontal disease (PD), which increase the overall “set point” of systemic inflammation, could modify the neuroinflammatory process^{20–24}. PD is a chronic and multifactorial inflammatory process caused by microorganisms and characterized by progressive destruction of the tooth-supporting apparatus, leading to tooth loss^{25,26}. Breakdown of periodontal tissues involves a complex interplay between the pathogenic bacteria, the microbial biofilm, and the host’s immune responses²⁷. During the establishment of PD, Gram-negative microorganisms increase up to 80%, colonize the gingival sulcus, form subgingival biofilm, and lead to the formation of periodontal pockets. In addition to aging and immunosenescence, chronic inflammation elicited by microbial infectious agents and their toxic products may also lead to aberrant microglia cell function^{13,14}. The cell wall components and various toxic products of periodontal pathogens can trigger the host response and induce destruction of periodontal tissues²⁸. Prevalence of PD is globally high making PD as one of the most common diseases²⁹. PD is highly associated with aging. Almost 47% of adults aged 30 years or older in the United States have PD³⁰. Chronic and systemically disseminating inflammation induced by PD is a risk factor for several conditions including stroke, cardiovascular diseases, diabetic complications, rheumatoid arthritis, and preterm birth³¹. A bi-directional link between AD and PD also has been suggested by cross-sectional human studies²¹. Tooth loss, which is a net result of progressive PD, was linked to cognitive decline and AD in the elderly^{32–36}. Furthermore, a study reported the association of higher brain amyloid load and PD in a cognitively normal elderly cohort³⁷. These studies demonstrate that PD results not only in the loss of bone support around the teeth but also in systemic inflammation; however, it is not known whether PD leads to changes in neuroinflammation nor the mechanism of PD-induced AD-associated pathologies.

In the present study, we tested the hypothesis that experimentally-induced PD in a mouse model of AD will impact the inflammatory process in the brain and microglia function. In contrast to other animal studies of PD that have used oral gavage or injections of human periodontal bacteria (e.g., *Porphyromonas gingivalis*), here we used a model of PD in which silk ligatures were placed on the maxillary second molars, resulting in the colonization of mouse oral bacteria and the development of PD rather than an introduction of a human pathogen. We thus examined differences in how ligature-induced PD results in alveolar bone loss and alters neuroinflammatory responses between AD-modeled mice and wild-type (WT) controls.

Results

Alveolar bone loss is higher in 5xFAD than in WT mice at baseline, and experimental PD increases bone loss in WT and 5xFAD mice. Silk ligatures were placed for four weeks on the maxillary second molars of 8-month-old 5xFAD and WT mice to induce PD. Since bone loss in the alveolus surrounding and supporting the teeth in the jaw is the hallmark of PD, we first measured the alveolar bone levels at baseline and after 4 weeks of placing the ligatures. As shown in Fig. 1A, the macroscopic examination of the maxilla of 5xFAD and WT littermates indicated that 5xFAD mice at baseline (not exposed to ligatures) had significantly higher levels of bone loss than WT littermates. After the induction of experimental PD, both 5xFAD and WT mice showed significantly increased bone loss, such that the difference between the bone loss area in 5xFAD and WT mice was no longer significant. Macroscopic findings were confirmed with histological measurements of alveolar bone levels in the furcation region of the maxillary molars in hematoxylin and eosin (H&E) stained sections (Fig. 1B).

To determine if the detected bone loss was associated with increased osteoclastic activity, maxillary sections were stained with tartrate resistant acid phosphatase (TRAP) (Fig. 1C). In parallel with the clinical and histological observations, TRAP+ osteoclastic cells at baseline were significantly increased in 5xFAD mice compared to WT mice, suggesting that the alveolar bone loss of 5xFAD mice was associated with increased osteoclastic activity. After ligature-induced PD was established, TRAP+ osteoclastic cell counts were significantly increased in WT mice while they were significantly decreased in 5xFAD mice.

Experimental PD increases insoluble A β 42 in 5xFAD mice. To test if inducing experimental PD in 5xFAD mice leads to increased A β pathology, we measured the levels of A β 40 and A β 42 in the TBS-soluble and -insoluble protein fractions of the prefrontal cortex by ELISA and also quantified the plaque burden in brain sections immunostained with antibodies to A β 42. The mean level of insoluble A β 42, but not A β 40, was significantly increased in ligature-treated 5xFAD mice compared to untreated 5xFAD mice (Fig. 2A). Differences of plaque burden measured in cortex, hippocampus, and dentate gyrus (DG) in ligature-treated and untreated 5xFAD mice were not significant (Fig. 2B).

Experimental PD differentially affects the activation state of microglia in WT and 5xFAD mice. We measured the impact of experimental PD on microglia activation in WT and 5xFAD mice by densitometric analysis of Iba1-immunostained brain sections. In WT mice, experimental PD led to significantly increased Iba1 levels in cortical layers 4–5 (CTX) and throughout the hippocampus, including the CA1, hippocampal fissure (HF), and DG (Fig. 3). As expected, 5xFAD mice had high levels of Iba1 immunostaining in cortex and hippocampus. Experimental PD in 5xFAD mice, however, did not lead to a further increase in Iba1 immunostaining and, in fact, resulted in a significant decrease in the DG compared to non-ligature 5xFAD mice.

Since function of activated microglia in AD depends on their association to A β plaques¹², we examined if experimental PD altered the density of PAMs in 5xFAD mice. We performed double fluorescent labeling of brain sections from 5xFAD mice with and without PD with Iba1 antibodies to visualize microglia and with thioflavin S (ThS) to stain amyloid fibrils (Fig. 4). Double-label fluorescent images of CTX were processed to determine

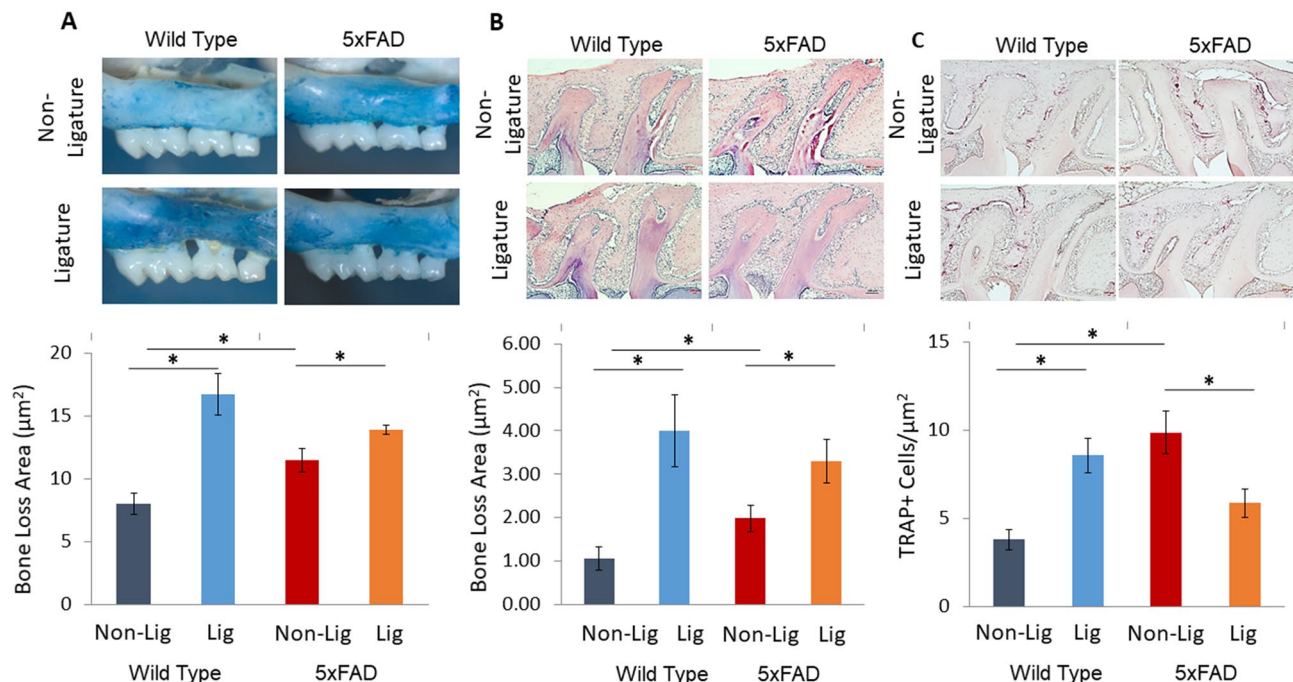


Figure 1. Experimental periodontitis and periodontal changes in a murine model of Alzheimer's disease. (A) 5xFAD mice at baseline (not exposed to ligatures; Non-Lig) had higher level of bone loss than WT littermates. After induction of experimental periodontitis by the placement of ligatures (Lig), 5xFAD and WT mice both showed significant bone loss while no significant differences were detected between the level of bone loss in ligature-treated 5xFAD mice and ligature-treated WT mice. (B) Macroscopic findings were confirmed with histological measurement of alveolar bone levels in furcation region of the maxillary molar. (C) TRAP stained osteoclastic cells were significantly increased in 5xFAD mice compared to the WT mice at baseline. (* $p < 0.05$).

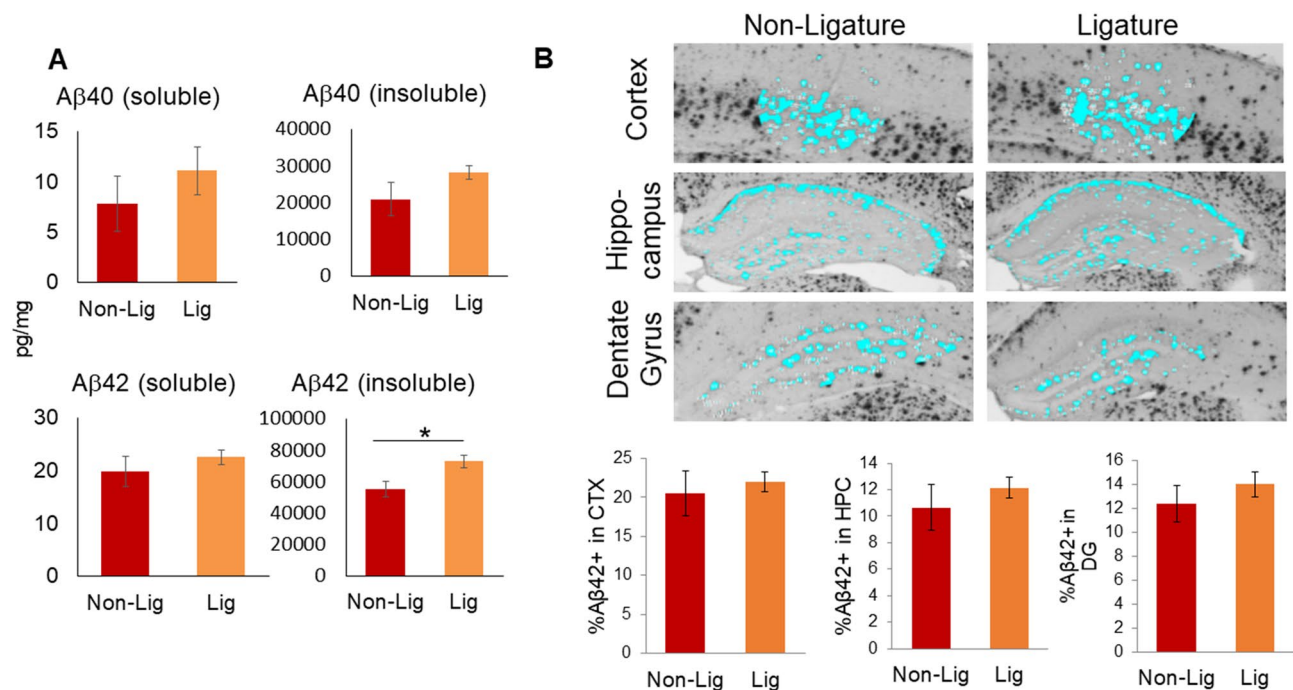


Figure 2. Amyloid beta ($\text{A}\beta$) accumulation and topographical distribution in the cortex, hippocampal formation, and dentate gyrus. (A) Soluble and insoluble forms of $\text{A}\beta$ in brain extracts from 5xFAD mice with (Lig) or without (Non-Lig) experimental PD. * $p < 0.05$ compared to non-PD animals. (B) Photomicrographs of $\text{A}\beta_{42}$ -immunostained sections containing cortical layers 4–5 (CTX), the hippocampus (HPC), and the dentate gyrus (DG) subregion of the hippocampus, were taken with a $4\times$ objective from Non-Lig and Lig 5xFAD mouse brain sections. A constant threshold was applied to each image. Analysis of all thresholded $\text{A}\beta_{42}$ particles was performed to obtain the percent area of $\text{A}\beta_{42}$ staining.

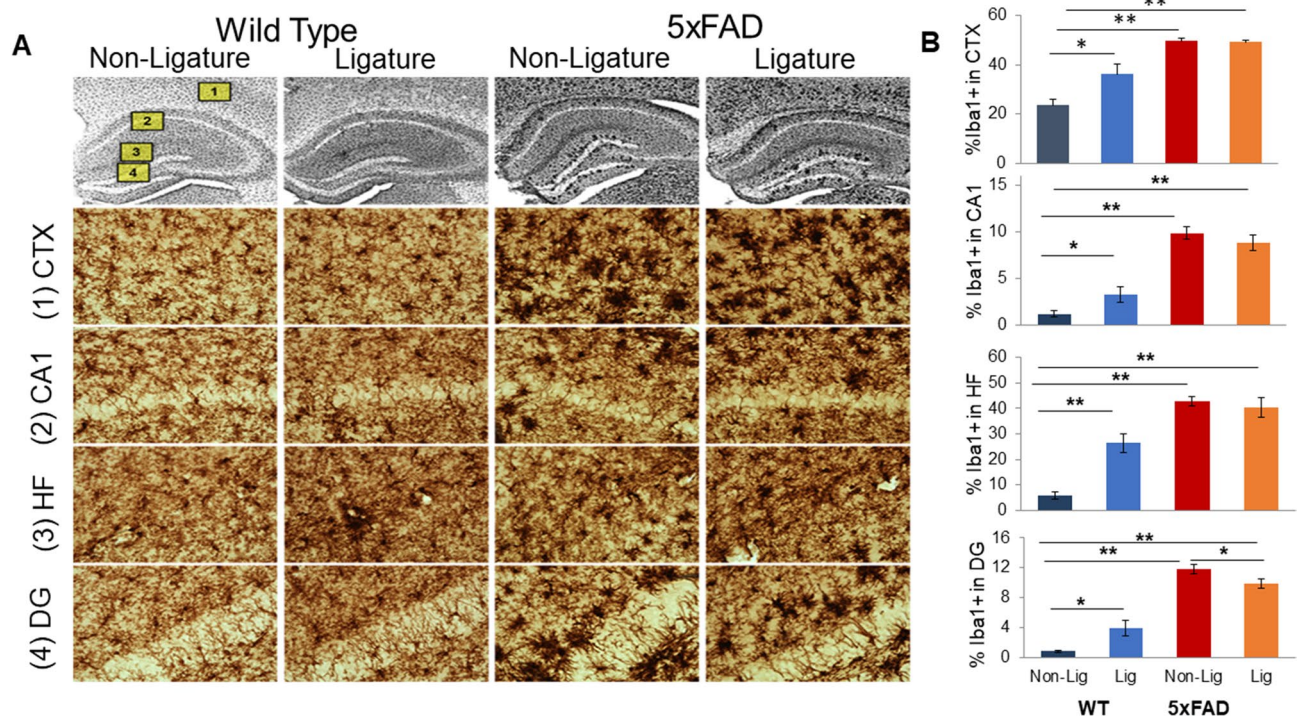


Figure 3. Impact of ligature-induced PD on microglia. **(A)** Photomicrographs of Iba1-immunostained sections from representative mouse brain sections at $\times 40$ magnification (top row). Insets on the first image indicate the magnified ($\times 400$) regions-of-interest (ROIs) displayed below as (1) cortical layers 4–5 (CTX), (2) hippocampal CA1, (3) hippocampal fissure (HF), and (4) hippocampal dentate gyrus (DG). **(B)** Average microglia densitometry was analyzed for each mouse group within the CTX, CA1, HF, and DG ROIs, respectively. Using photomicrographs magnified at $\times 100$, ROIs were outlined, a constant threshold was applied to each image, and analysis of all Iba1+ particles above the threshold was performed to obtain the percent area of Iba1+ staining (microglia densitometry). * $p < 0.05$, ** $p < 0.01$.

the total Iba1+ area of immunofluorescence and to define PAMs, as the percent area of Iba1 immunostaining in the immediate proximity ($6.5 \mu\text{m}$ perimeter) of each ThS+ accumulation. We found that the percentage of PAMs was significantly decreased in 5xFAD mice with PD compared to naïve 5xFAD mice (Fig. 4A), indicating that development of PD results in less clustering of microglia around amyloid plaques. Consistent with the data from single-label immunostaining of A β 42 (Fig. 2) and Iba1 (Fig. 3), there were no significant effects of experimental PD on total ThS fluorescence nor total Iba1 immunofluorescence (Fig. 4B).

Analysis of Brain Cytokines. We measured the concentration of cytokines in brain specimens of WT and 5xFAD mice with or without PD by multiplex immunoassay (Fig. 5). 5xFAD mice had significantly higher levels of TNF- α and IL-10 and lower levels of GM-CSF and IFN- γ in the brain samples compared to the WT controls in the absence of the placement of ligatures ($p < 0.05$). Ligature placement led to a significant reduction in IL-6, MCP-1, GM-CSF, and IFN- γ in brains of WT mice ($p < 0.05$) and in a significant reduction in IL-10 levels in 5xFAD mice ($p < 0.05$). MCP-1 levels in 5xFAD mice with PD were significantly higher than the WT mice ($p < 0.05$). When the ratio between TNF- α and IL-10 was compared as an index of inflammatory activation, 5xFAD mice showed a higher and unresolved inflammation in brain before and after the ligature placement compared to WT controls ($p < 0.05$).

Discussion

In this study, we tested the hypothesis that experimentally-induced periodontitis using the ligature model will have an effect on the neuroinflammatory process in a mouse model of AD. We used a well-established mouse model of AD, which is characterized by rapid A β accumulation, and studied the impact of the PD, which represents a complex infecto-inflammatory disease of the oral cavity. The results demonstrated that the AD-like condition alone leads to periodontal bone loss and that experimental PD differentially affects brain inflammation in mice with AD-like pathology and WT mice. Furthermore, our data points to an aberrant activation of microglia and dysregulation of the neuroinflammatory process that could underlie the mechanism of a PD-AD link.

PD has already been associated with several severe diseases of other organs in the body including the cardiovascular diseases, diabetes, rheumatoid arthritis, and pre-term birth³⁸. Recent data in humans has supported the premise that PD is associated with cognitive disorders and neuroinflammatory pathologies, including AD. In the context of pathological changes in the CNS associated with periodontal diseases in humans, the literature is growing, yet it is still not conclusive. A recent review summarized the current knowledge about the link between periodontal disease and cognitive disorders³⁹. A recent systematic review presented evidence that stroke may

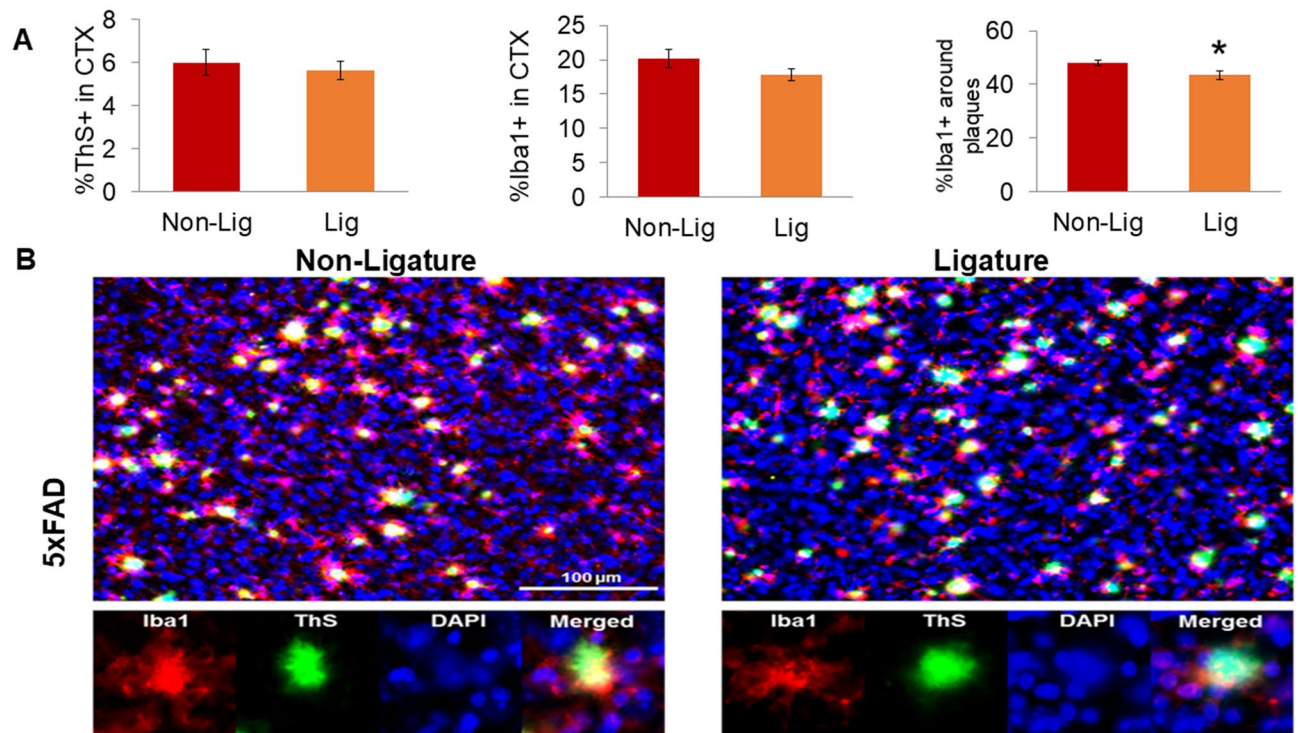


Figure 4. Impact of ligature-induced PD on plaque-associated microglia (PAMs) in 5xFAD mice. Fluorescent photomicrographs containing Iba1+ microglia (red), thioflavin S (ThS) dense-core plaques (green), and DAPI cell nuclei (blue) were taken of cortical layers 4–5 (CTX) from Non-Lig and Lig 5xFAD mice ($\times 20$ objective, 2 images/section, 3 sections/animal). Each fluorescent channel was automatically thresholded; an ROI around each ThS+ plaque (including a 6.5 μ m buffer-zone) was generated; and channels were analyzed within and without the ROI. (A) Dense-core plaque densitometry (%ThS+), microglia densitometry (%Iba1+), and the percentage of PAMs (%Iba1+ staining within the immediate proximity of ThS+ plaques), * $p < 0.05$. (B) Representative fluorescent photomicrographs of Non-Lig (left panels) and Lig (right panels) 5xFAD mouse cortex. Scale bar = 100 μ m. Bottom row: Iba1, ThS, DAPI, and merged channels from a representative image of a PAM.

be associated with poor oral health and periodontal disease⁴⁰. Oral bacteria (e.g., *Porphyromonas gingivalis*) and their enzymes have been detected in the brain of AD patients and were associated with neuroinflammation and amyloid-beta deposition^{28, 41}. Collectively, these studies suggest that in humans, the oral microbiome has an impact on brain pathology, cognitive decline, amyloid and tau-associated neurodegeneration and neuroinflammation. There are several models of PD currently used in the field⁴². One of the models often used to study murine experimental PD is the oral gavage model in which a human periodontal bacterium such as *Porphyromonas gingivalis* is inoculated orally, after treatment with antibiotics to suppress the mouse oral microbiota. Using this model of PD, there are reports showing an increase in markers associated with AD pathology and cognitive deficits^{43–46}. In the present study, we chose to use the ligature-induced model of PD. The advantage of the ligature-induced model over human-pathogen induced models is that a commensal mouse microbiome accumulates around silk ligatures placed around the mouse molars and colonize the periodontal space around the tooth. This leads to a switch in the pathogenicity of the periodontal microbiome as the species associated with periodontal disease dominate the microbial flora. Thus, as in humans, in the ligature-induced model, a transition from commensal to pathogenic microbiomes takes place in the periodontal tissue. The disease is mediated by an inflammatory process that in both humans and mice results in periodontal disease and tissue loss. As far as we know, this is the first study in a murine model that looks at the effect of ligature-induced PD in the brain.

There is also evidence that AD could be a risk for tooth loss and PD, suggesting a bi-directional effect between AD and PD^{13, 21, 24, 37, 47–50}. Our data suggest a bi-directional link between the AD and PD because 8-month-old 5xFAD mice presented a significantly higher level of bone loss prior to the placement of ligatures and the induction of experimental PD. After the induction of experimental PD both 5xFAD and WT mice showed a significant increase in bone loss. The data showed a reduced osteoclastic activity, as demonstrated by the number of preosteoclasts and osteoclasts stained positive for TRAP, in 5xFAD mice with PD, while osteoclastic activity was increased in WT mice with PD. This finding suggested that the peak bone resorption as a result of the inflammatory process in the periodontal tissues may have taken place earlier in 5xFAD mice compared to the WT littermates and therefore time-dependent experiments would be needed to further understand the effects of PD. Another explanation of this observation may be a biological mechanism where PD may induce changes in the immune system responses and stimulate immunosenescence^{51–53}, which could underlie the pathological process

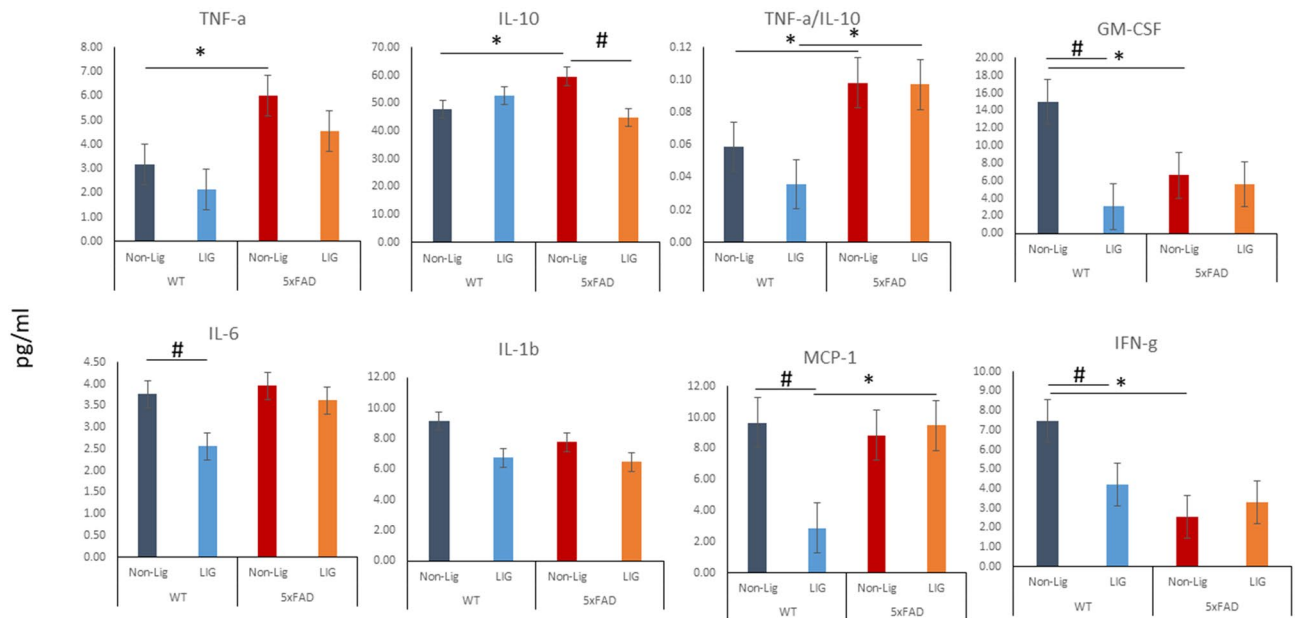


Figure 5. Cytokine profile of brain specimens in 5xFAD mice with or without ligature. Higher levels of TNF- α and IL-10, and lower levels of GM-CSF and IFN- γ in the 5xFAD mice brain samples compared to the WT controls were noted prior to the placement of ligatures. There was a significant reduction in IL-6, MCP-1, GM-CSF, and IFN- γ in brains of WT mice and IL-10 in 5xFAD mice after ligature placement. MCP-1 levels in ligated 5xFAD mice were significantly higher than in ligated WT mice. 5xFAD mice showed a higher and unresolved inflammation (TNF- α /IL-10 ratio) compared to WT controls (* $p < 0.05$, compared to WT animals; # $p < 0.05$, compared to non-ligature group; ANOVA with posthoc analysis for multiple comparison).

in AD. Evaluating the effects of ligature-induced PD in 5xFAD mice at earlier ages or in a slow-progressing AD models (e.g., PSAPP), may demonstrate the role of A β pathology in the link between AD and PD.

One of the key findings from this study is that experimental PD had an impact on microglia and the brain's cytokine profile. The risk of developing PD increases with age; however, PD has a peak rate of occurrence in middle age that may result in priming microglia to a significantly activated state increasing the brain vulnerability to aging and to additional immune challenges or diseases. While microglia in WT mice was impacted by the experimental PD as shown by increased Iba1 expression, the level of inflammatory cytokines was also impacted, suggesting a defective immunological process due to PD^{51–53} that would lead to a disrupted inflammatory response. As PD can prime macrophages either through microbial factors (e.g., lipopolysaccharide)^{54, 55} or by activation of other immune and non-immune cells^{56, 57}, microglia priming, activation, and polarization due to PD may be plausible²⁴. The exaggerated response of primed microglia is known to contribute to the pathogenesis of AD⁵⁸. In contrast to our previous study where we reported a significant increase in the level of some inflammatory cytokines (GM-CSF, IL-6, IFN- γ , and IL-1 β) in 3-month-old 5xFAD mice³, in the current study using 8-month-old 5xFAD mice, these specific cytokines were not increased. Although we did not expect these results, a dynamic change of cytokines and pattern of different inflammatory markers throughout the disease course have been reported. For example, a very recent work⁵⁹ suggested that microglia expressed multiple inflammatory profiles that change from 3 to 12 months of age and are associated with their protective response to accumulating A β plaques in the more slowly progressing APP/PS1 mouse model of AD. One study⁶⁰ has raised the possibility that deposition of A β plaques initially buffer or diminish the brain immune response to the insult. Additional longitudinal studies will be necessary to evaluate this idea to understand this apparent discrepancy. Ligature-induced PD disrupts the brain's cytokine profile especially in WT mice. As presented in Fig. 5, PD reduces the levels of IL-6, MCP-1, IFN- γ and GM-CSF in the brain of WT mice. Increasing number of studies support the concept that inflammatory dysregulation and cytokine imbalance is associated with neurodegenerative dementias⁶¹ and that rebalancing the activation of the innate immune system instead of suppressing it represent a new therapeutic approach. Therefore, the immune dysregulation that we detect after the development of PD may be of great significance and it will have to be further investigated.

In parallel with the increased insoluble A β 42 levels, there was a significant decrease in plaque-associated microglia (PAMs) in 5xFAD animals with experimentally induced PD. This important finding suggests that the additional inflammatory challenge caused by PD results in a failure of microglia to function as a protective barriers around plaques, which opens hot spots around the plaques that result in the destabilization of plaques and the increased neurotoxicity⁶². Contrasting with the protective role of PAMs in A β phagocytosis and in preventing neuronal damage, dysfunctional PAMs can induce further neuroinflammation that disrupt non-PAMs microglia and other cells throughout the brain⁶³. Thus, the effect of PD on PAMs can cause a significant modulation of neuroinflammation. Indeed, this observation was further supported by our findings that PD results in an aberrant profile of cytokines and chemokines, indicating a dysfunctional regulation of neuroinflammation in AD. While

microglia cells ultimately become dysfunctional under AD conditions, the additional “hit” of PD may occupy some microglia to prevent PAMs from forming. Alternatively, PD might prime microglia such that they become more rapidly hyperactive and dysfunctional as AD pathology accumulates. Both of these possibilities, while further exploration is necessary, are highly plausible based on our findings that PD directly increases microglia activation, which was especially obvious in WT mice.

Our findings point to microglia as being a crucial link between the inflammation induced by PD and accelerated AD pathology. PD has been shown to result in a disruption in the inflammation and cytokine levels in brain. Since bacteria may infiltrate the central nervous system, which can directly activate microglia and indirectly via reactive astrocytes, PD may change the set-point of inflammatory modification of blood–brain-barrier and lead to a “leaky” barrier function. The mechanism of this effect is not known; however, the data clearly places PD at a risk level of that seen in other systemic inflammatory processes and suggests the possibility that oral microorganisms, which can cause systemic inflammation, should be regarded with the similar risk profile as the gut microbiome.

Collectively, we demonstrated that the alveolar bone loss was higher in 5xFAD than in WT mice at baseline, experimental PD increased bone loss in both 5xFAD and WT mice, experimental PD increased insoluble A β 42 in 5xFAD mice and modified the microglia activation in both WT and 5xFAD mice, and experimental PD results in an aberrant inflammatory regulation in the brains of 5xFAD mice suggesting a distinct neuroinflammatory response to experimental PD in WT and 5xFAD mice and therefore a potential mechanism that can link PD and AD.

Materials and methods

Mice. Eight-month old male 5xFAD (n = 15) and non-transgenic male littermate (WT; n = 15) mice were used in the study. 5xFAD mice co-express human APP and PS1 with multiple FAD mutations [APP K670N/M671L (Swedish) + I716V (Florida) + V717I (London) and PS1 M146L + L286V] with specific neuronal expression driven by the Thy-1 promoter⁶⁴. Eight mice in each group (WT or 5xFAD) were treated with ligatures to induce experimental PD while seven mice per group were left untreated.

Experimental periodontitis in mice. Ligature-induced PD was established after placement of silk monofilament threads corresponding to 7.0-thickness (Perma-Hand silk, black braided Ethicon A182). The ligature was placed subgingivally on the maxillary right and left second molars with fine microsurgical instruments under ketamine (80 mg/kg, i.p.) and xylazine (16 mg/kg, i.p.) anesthesia. PD developed and reached chronicity in 4 weeks. The mice were weighed weekly during the study to assess health status and no differences in weight were detected between mice treated with ligatures and those left untreated. All animal experiments were carried in accordance with the NIH Guide for the Care and Use of Laboratory Animals and were approved by the local animal care committee at the Forsyth Institute.

Assessment of periodontal disease and alveolar bone loss. After euthanasia, the maxillae were dissected free of muscle and soft tissue, keeping the attached gingiva intact. The maxilla was then split into two halves from the midline between the central incisors. The right half was taken for morphometric analysis and the left half was used for histological evaluation. For morphometric analysis, the right maxilla was defleshed and stained with methylene blue for the visual distinction between the tooth and bone based on the absorption of the blue dye by the two hard tissues with different calcification⁶⁵. The bone level was quantified using Image Analysis (Image-Pro Plus 4.0; Media Cybernetics).

Histomorphometric assessment of periodontal bone loss. The left half of the maxilla was decalcified and embedded in paraffin as described before⁶⁶. Thin sections (5 μ m) were cut and stained either with H&E for light microscopy and identification of the histological bone loss or with tartrate-resistant acid phosphatase (TRAP) to measure the osteoclastic activity as a reflection of number of preosteoclasts and osteoclasts stained positive for TRAP⁶⁷. To further quantify the changes in the bone at the histological level, the mean value (\pm SD) of the linear distance and the area of bone loss was calculated as we have previously published⁶⁶. A previously developed measurement technique was used to calculate the bone changes at three different sections of the root^{66,68}. Linear distance was reported as the distance from the base of the epithelium to the alveolar crest border at the apical, middle, and the coronal third of the root and expressed as the difference between 5xFAD and WT animals. Area measurements were presented as the difference between the total area. Osteoclastogenesis was examined in TRAP-stained sections by counting the osteoclasts. 3,3'-diaminobenzidine tetrahydrochloride (DAB)-stained slides were counterstained with hematoxylin. Images were acquired and analyzed using the Nikon Eclipse 80i microscope and Northern Eclipse Imaging Elements-D (NIS-D) software. Results were expressed as percent of total positive cells.

Brain collection and processing. After euthanasia, brains were collected. The left hemisphere was post-fixed with 4% paraformaldehyde solution for 24 h and cryoprotected in a graded series of 10% and 20% glycerol/2% DMSO solution for the immunohistological analysis of microglia and A β plaques. The prefrontal cortex of the right hemisphere was dissected for the analysis of A β levels by ELISA and for the levels of inflammatory cytokines and chemokines.

Analysis of A β deposits and microglia by immunohistochemistry. Cryoprotected hemibrains were serially cut at 50 μ m on a freezing microtome and were immunostained with specific antibodies, as described⁶⁹. Anti-A β 1–42 (Invitrogen #700254, 1:1000) was used to define A β deposits and anti-Iba1 was used to stain

microglia (Wako Chemicals #019-19741; 1:5000). In brief, free-floating sections were incubated overnight in primary antibody followed by PBS (Phosphate buffered saline) washes and incubation in peroxidase-conjugated secondary antibody followed by development using 3'-diaminobenzidine tetrahydrochloride (DAB) as a chromagen. Three serial sections per subject, 0.5 mm apart from each other were quantified in a blinded manner. Quantification of A β and Iba1 immunostaining was performed by densitometry using the threshold function on NIH Image J.

Double-label fluorescent analysis of plaque-associated microglia (PAMs). A series of brain sections underwent a 30 min antigen retrieval incubation at 60 °C in citrate buffer, followed by counterstaining of plaques, in which sections were incubated in 0.01% thioflavin S (ThS) in 40% ethanol for 45 min and then differentiated in 3 min with 40% ethanol. Sections then underwent immunostaining using the Iba1 primary antibody and a fluorescently-tagged secondary antibody (1:200 Texas Red goat anti-rabbit, Vector Labs) to label microglia and fluorescent staining of cell nuclei using DAPI. Multi-channel images of cortical layers 4–5 (2 images/section, 3 sections/animal) were taken using a 20 \times objective on a fluorescent microscope (Nikon Eclipse 50i). Images were processed using NIH ImageJ by automatically thresholding the image of each channel and measuring the densitometry (% area) of Iba1 within the local proximity of ThS+ plaques (plaque-associated microglia, within a 6.4 μ m enlarged radius of ThS staining) and within the space between plaques (non-plaque associated microglia).

Analysis of A β levels by ELISA. Dissected pre-frontal cortex was homogenized with 10 volumes (w/v) of Tris-buffered saline (TBS) and centrifuged at 100,000g for 1 h at 4 °C. After saving the soluble supernatant fraction, the resulting pellet was re-suspended with 10 volumes of cold 5 M guanidine HCl buffer and saved as the insoluble fraction. Specific human A β 40 and A β 42 ELISA kits (Invitrogen, cat# KHB 3544 and KHB 3545) were used to analyze the soluble and insoluble tissue fractions according to the manufacturer's specifications and as previously described³.

Analysis of brain inflammatory cytokines and chemokines. Cortical brain homogenates were analyzed for a panel of inflammatory cytokines and chemokines (GM-CSF, IFN- γ , IL-1 β , IL-6, IL-10, TNF- α , MCP-1) using the multiplex immunoassay, according to the manufacturer's specifications (Millipore Sigma; MCYTOMAG-70 K) and as previously described³. The results were read on Bio-Plex 200 following manufacturers' specifications and using Bio-Plex Manager software version 6.0 (Bio-Rad Laboratories, Hercules, CA).

Received: 18 April 2020; Accepted: 30 September 2020

Published online: 29 October 2020

References

1. Blennow, K., de Leon, M. J. & Zetterberg, H. Alzheimer's disease. *Lancet* **368**, 387–403. [https://doi.org/10.1016/S0140-6736\(06\)69113-7](https://doi.org/10.1016/S0140-6736(06)69113-7) (2006).
2. Akiyama, H. *et al.* Inflammation and Alzheimer's disease. *Neurobiol. Aging* **21**, 383–421 (2000).
3. Kantarci, A. *et al.* Combined administration of resolvin E1 and lipoxin A4 resolves inflammation in a murine model of Alzheimer's disease. *Exp. Neurol.* **300**, 111–120. <https://doi.org/10.1016/j.expneurol.2017.11.005> (2018).
4. Streit, W. J., Xue, Q. S., Tischer, J. & Bechmann, I. Microglial pathology. *Acta Neuropathol. Commun.* **2**, 142. <https://doi.org/10.1186/s40478-014-0142-6> (2014).
5. Perry, V. H., Nicoll, J. A. & Holmes, C. Microglia in neurodegenerative disease. *Nat. Rev. Neurol.* **6**, 193–201. <https://doi.org/10.1038/nrneuro.2010.17> (2010).
6. Shaked, I., Porat, Z., Gersner, R., Kipnis, J. & Schwartz, M. Early activation of microglia as antigen-presenting cells correlates with T cell-mediated protection and repair of the injured central nervous system. *J. Neuroimmunol.* **146**, 84–93. <https://doi.org/10.1016/j.jneuroim.2003.10.049> (2004).
7. Sierra, A. *et al.* Surveillance, phagocytosis, and inflammation: How never-resting microglia influence adult hippocampal neurogenesis. *Neural Plast.* **2014**, 610343. <https://doi.org/10.1155/2014/610343> (2014).
8. El Khoury, J. *et al.* Ccr2 deficiency impairs microglial accumulation and accelerates progression of Alzheimer-like disease. *Nat. Med.* **13**, 432–438. <https://doi.org/10.1038/nm1555> (2007).
9. Streit, W. J. Microglia and Alzheimer's disease pathogenesis. *J. Neurosci. Res.* **77**, 1–8. <https://doi.org/10.1002/jnr.20093> (2004).
10. Streit, W. J., Braak, H., Xue, Q. S. & Bechmann, I. Dystrophic (senescent) rather than activated microglial cells are associated with tau pathology and likely precede neurodegeneration in Alzheimer's disease. *Acta Neuropathol.* **118**, 475–485. <https://doi.org/10.1007/s00401-009-0556-6> (2009).
11. Hickman, S. E., Allison, E. K. & El Khoury, J. Microglial dysfunction and defective beta-amyloid clearance pathways in aging Alzheimer's disease mice. *J. Neurosci.* **28**, 8354–8360. <https://doi.org/10.1523/JNEUROSCI.0616-08.2008> (2008).
12. Condello, C., Yuan, P., Schain, A. & Grutzendler, J. Microglia constitute a barrier that prevents neurotoxic protofibrillar Abeta42 hotspots around plaques. *Nat. Commun.* **6**, 6176. <https://doi.org/10.1038/ncomms7176> (2015).
13. Stephenson, J., Nutma, E., van der Valk, P. & Amor, S. Inflammation in CNS neurodegenerative diseases. *Immunology* **154**, 204–219. <https://doi.org/10.1111/imm.12922> (2018).
14. Labzin, L. I., Heneka, M. T. & Latz, E. Innate immunity and neurodegeneration. *Annu. Rev. Med.* **69**, 437–449. <https://doi.org/10.1146/annurev-med-050715-104343> (2018).
15. Perry, V. H., Cunningham, C. & Holmes, C. Systemic infections and inflammation affect chronic neurodegeneration. *Nat. Rev. Immunol.* **7**, 161–167. <https://doi.org/10.1038/nri2015> (2007).
16. Perry, V. H. & Teeling, J. Microglia and macrophages of the central nervous system: The contribution of microglia priming and systemic inflammation to chronic neurodegeneration. *Semin. Immunopathol.* **35**, 601–612. <https://doi.org/10.1007/s00281-013-0382-8> (2013).
17. Lim, S. L., Rodriguez-Ortiz, C. J. & Kitazawa, M. Infection, systemic inflammation, and Alzheimer's disease. *Microbes Infect.* **17**, 549–556. <https://doi.org/10.1016/j.micinf.2015.04.004> (2015).
18. Magalhaes, T. N. C. *et al.* Systemic inflammation and multimodal biomarkers in amnesic mild cognitive impairment and Alzheimer's disease. *Mol. Neurobiol.* **55**, 5689–5697. <https://doi.org/10.1007/s12035-017-0795-9> (2018).

19. Holmes, C. & Butchart, J. Systemic inflammation and Alzheimer's disease. *Biochem. Soc. Trans.* **39**, 898–901. <https://doi.org/10.1042/BST0390898> (2011).
20. Miklosy, J. Emerging roles of pathogens in Alzheimer disease. *Expert Rev. Mol. Med.* **13**, e30. <https://doi.org/10.1017/S146239941002006> (2011).
21. Kamer, A. R. *et al.* Inflammation and Alzheimer's disease: Possible role of periodontal diseases. *Alzheimer's Dement. J. Alzheimer's Assoc.* **4**, 242–250. <https://doi.org/10.1016/j.jalz.2007.08.004> (2008).
22. Kamer, A. R. *et al.* Alzheimer's disease and peripheral infections: The possible contribution from periodontal infections, model and hypothesis. *J. Alzheimers Dis.* **13**, 437–449 (2008).
23. Miklosy, J. Alzheimer's disease—a neurospirochetosis. Analysis of the evidence following Koch's and Hill's criteria. *J. Neuroinflamm.* **8**, 90. <https://doi.org/10.1186/1742-2094-8-90> (2011).
24. Singhrao, S. K. *et al.* Oral inflammation, tooth loss, risk factors, and association with progression of Alzheimer's disease. *J. Alzheimer's Dis. JAD* **42**, 723–737. <https://doi.org/10.3233/JAD-140387> (2014).
25. Preshaw, P. M., Seymour, R. A. & Heasman, P. A. Current concepts in periodontal pathogenesis. *Dental Update* **31**(570–572), 574–578. <https://doi.org/10.12968/denu.2004.31.10.570> (2004).
26. Papapanou, P. N. Periodontal diseases: Basic concepts, association with systemic health, and contemporary studies of pathobiology. *Ann. R. Aust. Coll. Dent. Surg.* **21**, 33–42 (2012).
27. Benakanakere, M. & Kinane, D. F. Innate cellular responses to the periodontal biofilm. *Front. Oral Biol.* **15**, 41–55. <https://doi.org/10.1159/000329670> (2012).
28. Dominy, S. S. *et al.* Porphyromonas gingivalis in Alzheimer's disease brains: Evidence for disease causation and treatment with small-molecule inhibitors. *Sci. Adv.* **5**, eaau3333. <https://doi.org/10.1126/sciadv.aau3333> (2019).
29. Nazir, M. A. Prevalence of periodontal disease, its association with systemic diseases and prevention. *Int. J. Health Sci.* **11**, 72–80 (2017).
30. Armitage, G. C. Periodontal diagnoses and classification of periodontal diseases. *Periodontology* **2000**(34), 9–21 (2004).
31. Genco, R. J. & Borgnakke, W. S. Risk factors for periodontal disease. *Periodontology* **2000**(62), 59–94. <https://doi.org/10.1111/1/j.1600-0757.2012.00457.x> (2013).
32. Gatz, M. *et al.* Potentially modifiable risk factors for dementia in identical twins. *Alzheimer's Dement. J. Alzheimer's Assoc.* **2**, 110–117. <https://doi.org/10.1016/j.jalz.2006.01.002> (2006).
33. Stein, P. S., Desrosiers, M., Donegan, S. J., Yepes, J. F. & Kryscio, R. J. Tooth loss, dementia and neuropathology in the Nun study. *J. Am. Dent. Assoc.* **138**, 1314–1322 (2007) (quiz 1381–1312).
34. Minn, Y. K. *et al.* Tooth loss is associated with brain white matter change and silent infarction among adults without dementia and stroke. *J. Korean Med. Sci.* **28**, 929–933. <https://doi.org/10.3346/jkms.2013.28.6.929> (2013).
35. Li, J., Xu, H., Pan, W. & Wu, B. Association between tooth loss and cognitive decline: A 13-year longitudinal study of Chinese older adults. *PLoS ONE* **12**, e0171404. <https://doi.org/10.1371/journal.pone.0171404> (2017).
36. Heneka, M. T., Kummer, M. P. & Latz, E. Innate immune activation in neurodegenerative disease. *Nat. Rev. Immunol.* **14**, 463–477. <https://doi.org/10.1038/nri3705> (2014).
37. Kamer, A. R. *et al.* Periodontal disease associates with higher brain amyloid load in normal elderly. *Neurobiol. Aging* **36**, 627–633. <https://doi.org/10.1016/j.neurobiolaging.2014.10.038> (2015).
38. Sabharwal, A., Gomes-Filho, I. S., Stellrecht, E. & Scannapieco, F. A. Role of periodontal therapy in management of common complex systemic diseases and conditions: An update. *Periodontology* **2000**(78), 212–226. <https://doi.org/10.1111/prd.12226> (2018).
39. Wang, R. P., Ho, Y. S., Leung, W. K., Goto, T. & Chang, R. C. Systemic inflammation linking chronic periodontitis to cognitive decline. *Brain Behav. Immun.* **81**, 63–73. <https://doi.org/10.1016/j.bbi.2019.07.002> (2019).
40. Pillai, R. S. *et al.* Oral health and brain injury: Causal or casual relation?. *Cerebrovasc. Dis. Extra* **8**, 1–15. <https://doi.org/10.1159/000484989> (2018).
41. Olsen, I. & Singhrao, S. K. Porphyromonas gingivalis infection may contribute to systemic and intracerebral amyloid-beta: implications for Alzheimer's disease onset. *Expert. Rev. Anti Infect. Ther.* <https://doi.org/10.1080/14787210.2020.1792292> (2020).
42. Abe, T. & Hajishengallis, G. Optimization of the ligature-induced periodontitis model in mice. *J. Immunol. Methods* **394**, 49–54. <https://doi.org/10.1016/j.jim.2013.05.002> (2013).
43. Ilievski, V. *et al.* Chronic oral application of a periodontal pathogen results in brain inflammation, neurodegeneration and amyloid beta production in wild type mice. *PLoS ONE* **13**, e0204941. <https://doi.org/10.1371/journal.pone.0204941> (2018).
44. Ding, Y., Ren, J., Yu, H., Yu, W. & Zhou, Y. Porphyromonas gingivalis, a periodontitis causing bacterium, induces memory impairment and age-dependent neuroinflammation in mice. *Immun. Ageing I A* **15**, 6. <https://doi.org/10.1186/s12979-017-0110-7> (2018).
45. Ishida, N. *et al.* Periodontitis induced by bacterial infection exacerbates features of Alzheimer's disease in transgenic mice. *NPJ Aging Mech. Dis.* **3**, 15. <https://doi.org/10.1038/s41514-017-0015-x> (2017).
46. Poole, S. *et al.* Active invasion of Porphyromonas gingivalis and infection-induced complement activation in ApoE^{-/-} mice brains. *J. Alzheimer's Dis. JAD* **43**, 67–80. <https://doi.org/10.3233/JAD-140315> (2015).
47. Teixeira, F. B. *et al.* Periodontitis and Alzheimer's disease: A possible comorbidity between oral chronic inflammatory condition and neuroinflammation. *Front. Aging Neurosci.* **9**, 327. <https://doi.org/10.3389/fnagi.2017.00327> (2017).
48. Harding, A., Robinson, S., Crean, S. & Singhrao, S. K. Can better management of periodontal disease delay the onset and progression of Alzheimer's disease?. *J. Alzheimer's Dis. JAD* **58**, 337–348. <https://doi.org/10.3233/JAD-170046> (2017).
49. Kamer, A. R. *et al.* Periodontal disease's contribution to Alzheimer's disease progression in Down syndrome. *Alzheimers Dement. (Amst.)* **2**, 49–57. <https://doi.org/10.1016/j.dadm.2016.01.001> (2016).
50. Olsen, I. & Singhrao, S. K. Can oral infection be a risk factor for Alzheimer's disease?. *J. Oral Microbiol.* **7**, 29143. <https://doi.org/10.3402/jom.v7.29143> (2015).
51. Ebersole, J. L. *et al.* Age and periodontal health—immunological view. *Curr. Oral Health Rep.* **5**, 229–241. <https://doi.org/10.1007/s40496-018-0202-2> (2018).
52. Preshaw, P. M., Henne, K., Taylor, J. J., Valentine, R. A. & Conrads, G. Age-related changes in immune function (immune senescence) in caries and periodontal diseases: A systematic review. *J. Clin. Periodontol.* **44**(Suppl 18), S153–S177. <https://doi.org/10.1111/jcpe.12675> (2017).
53. Ebersole, J. L. *et al.* Aging, inflammation, immunity and periodontal disease. *Periodontology* **2000**(72), 54–75. <https://doi.org/10.1111/prd.12135> (2016).
54. Cecil, J. D. *et al.* Outer membrane vesicles prime and activate macrophage inflammasomes and cytokine secretion in vitro and in vivo. *Front. Immunol.* **8**, 1017. <https://doi.org/10.3389/fimmu.2017.01017> (2017).
55. Belfield, L. A., Bennett, J. H., Abate, W. & Jackson, S. K. Exposure to Porphyromonas gingivalis LPS during macrophage polarization leads to diminished inflammatory cytokine production. *Arch. Oral Biol.* **81**, 41–47. <https://doi.org/10.1016/j.archoralbi.2017.04.021> (2017).
56. Feghali, K. & Grenier, D. Priming effect of fibronectin fragments on the macrophage inflammatory response: Potential contribution to periodontitis. *Inflammation* **35**, 1696–1705. <https://doi.org/10.1007/s10753-012-9487-9> (2012).
57. Tzsch-Nahman, R. *et al.* Oral fibroblasts modulate the macrophage response to bacterial challenge. *Sci. Rep.* **7**, 11516. <https://doi.org/10.1038/s41598-017-11771-3> (2017).
58. Li, J. W., Zong, Y., Cao, X. P., Tan, L. & Tan, L. Microglial priming in Alzheimer's disease. *Ann. Transl. Med.* **6**, 176. <https://doi.org/10.21037/atm.2018.04.22> (2018).

59. Liu, L. *et al.* Multiple inflammatory profiles of microglia and altered neuroimages in APP/PS1 transgenic AD mice. *Brain Res. Bull.* **156**, 86–104. <https://doi.org/10.1016/j.brainresbull.2020.01.003> (2020).
60. Meyer, P. F. *et al.* Bi-directional association of cerebrospinal fluid immune markers with stage of Alzheimer's disease pathogenesis. *J. Alzheimer's Dis. JAD* **63**, 577–590. <https://doi.org/10.3233/JAD-170887> (2018).
61. Taipale, R. *et al.* Proinflammatory and anti-inflammatory cytokines in the CSF of patients with Alzheimer's disease and their correlation with cognitive decline. *Neurobiol. Aging* **76**, 125–132. <https://doi.org/10.1016/j.neurobiolaging.2018.12.019> (2019).
62. Minagar, A. *et al.* The role of macrophage/microglia and astrocytes in the pathogenesis of three neurologic disorders: HIV-associated dementia, Alzheimer disease, and multiple sclerosis. *J. Neurol. Sci.* **202**, 13–23. [https://doi.org/10.1016/s0022-510x\(02\)00207-1](https://doi.org/10.1016/s0022-510x(02)00207-1) (2002).
63. Navarro, V. *et al.* Microglia in Alzheimer's disease: Activated, dysfunctional or degenerative. *Front. Aging Neurosci.* **10**, 140. <https://doi.org/10.3389/fnagi.2018.00140> (2018).
64. Oakley, H. *et al.* Intraneuronal beta-amyloid aggregates, neurodegeneration, and neuron loss in transgenic mice with five familial Alzheimer's disease mutations: Potential factors in amyloid plaque formation. *J. Neurosci.* **26**, 10129–10140. <https://doi.org/10.1523/JNEUROSCI.1202-06.2006> (2006).
65. Hasturk, H. *et al.* Resolvin E1 regulates inflammation at the cellular and tissue level and restores tissue homeostasis in vivo. *J. Immunol.* **179**, 7021–7029 (2007).
66. Papathanasiou, E., Kantarci, A., Konstantinidis, A., Gao, H. & Van Dyke, T. E. SOCS-3 regulates alveolar bone loss in experimental periodontitis. *J. Dent. Res.* **95**, 1018–1025. <https://doi.org/10.1177/0022034516645332> (2016).
67. Minkin, C. Bone acid phosphatase: Tartrate-resistant acid phosphatase as a marker of osteoclast function. *Calcif. Tissue Int.* **34**, 285–290 (1982).
68. Hasturk, H. *et al.* RvE1 protects from local inflammation and osteoclast-mediated bone destruction in periodontitis. *FASEB J.* **20**, 401–403. <https://doi.org/10.1096/fj.05-4724fje> (2006).
69. Kowall, N. W. *et al.* MPTP induces alpha-synuclein aggregation in the substantia nigra of baboons. *NeuroReport* **11**, 211–213 (2000).

Acknowledgements

This research was supported by grants from the NIH/NIA (R01AG062496 to A. Dedeoglu and A. Kantarci) and the Department of Veteran Affairs (Merit Award BX001875 to A. Dedeoglu).

Author contributions

A.K. and A.D. conceived the idea, oversaw all aspects of the work, provided the funding. C.M.T., W.Y., A.M., D.S., and J.-Y.A. worked on several aspects of the experiments. I.C. worked on the design and oversight of experimental work. All authors contributed to the data evaluation, manuscript preparation.

Competing interests

The authors declare no competing interests.

Additional information

Correspondence and requests for materials should be addressed to A.D.

Reprints and permissions information is available at www.nature.com/reprints.

Publisher's note Springer Nature remains neutral with regard to jurisdictional claims in published maps and institutional affiliations.



Open Access This article is licensed under a Creative Commons Attribution 4.0 International License, which permits use, sharing, adaptation, distribution and reproduction in any medium or format, as long as you give appropriate credit to the original author(s) and the source, provide a link to the Creative Commons licence, and indicate if changes were made. The images or other third party material in this article are included in the article's Creative Commons licence, unless indicated otherwise in a credit line to the material. If material is not included in the article's Creative Commons licence and your intended use is not permitted by statutory regulation or exceeds the permitted use, you will need to obtain permission directly from the copyright holder. To view a copy of this licence, visit <http://creativecommons.org/licenses/by/4.0/>.

© The Author(s) 2020